Inactivation of the Sodium Channel

I. Sodium Current Experiments

FRANCISCO BEZANILLA and CLAY M. ARMSTRONG

From the Department of Physiology, University of Pennsylvania, School of Medicine, Philadelphia, Pennsylvania 19174

ABSTRACT Inactivation of sodium conductance has been studied in squid axons with voltage clamp techniques and with the enzyme pronase which selectively destroys inactivation. Comparison of the sodium current before and after pronase treatment shows a lag of several hundred microseconds in the onset of inactivation after depolarization. This lag can also be demonstrated with double-pulse experiments. When the membrane potential is hyperpolarized to −140 mV before depolarization, both activation and inactivation are delayed. These findings suggest that inactivation occurs only after activation; i.e. that the channels must open before they can inactivate. The time constant of inactivation measured with two pulses (τ_c) is the same as the one measured from the decay of the sodium current during a single pulse (τ_h). For large depolarizations, steady-state inactivation becomes more incomplete as voltage increases; but it is relatively complete and appears independent of voltage when determined with a two-pulse method. This result confirms the existence of a second open state for Na channels, as proposed by Chandler and Meves (1970. J. Physiol. [Lond.]. **211**:653–678). The time constant of recovery from inactivation is voltage dependent and decreases as the membrane potential is made more negative. A model for Na channels is presented which has voltage-dependent transitions between the closed and open states, and a voltage-independent transition between the open and the inactivated state. In this model the voltage dependence of inactivation is a consequence of coupling to the activation process.

INTRODUCTION

Each sodium channel of the squid axon membrane is controlled by two gates, Na activation and Na inactivation, both of which must be open for a channel to conduct (14). The activation gate has quick kinetics when both opening and closing. It is closed at rest, but opens quickly after depolarization, and produces the very fast P_{Na} increase that initiates the action potential. The activation gate closes quickly on repolarization. The inactivation gate operates more slowly and has the opposite voltage dependence: it is open at rest, closes slowly on depolarization, and opens slowly on repolarization. This gate cuts short the P_{Na} increase that is initiated by opening the activation gate, and it makes repolarization to the resting potential (by opening of the K channels) easier. Closed inactivation gates after a depolarization are an important factor in the refractory period.

Kinetic evidence for the existence of two gates on each Na channel is strong (13), and has been confirmed by internal perfusion of axons with pronase, which destroys inactivation while leaving activation intact (4).

In the Hodgkin and Huxley formulation, activation and inactivation gates were made (partly for computational ease) completely independent. That is, each gate can open and close regardless of the condition of the other gate. Hoyt (15, 16) has pointed out that the gates may be coupled in some way rather than being entirely independent. Subsequent to this investigator's suggestion it has been shown that inactivation after depolarization follows a lag that is not predicted by the Hodgkin and Huxley (14) equations (1, 10; see below). This delay indicates that some change must take place in the membrane before inactivation begins, but does not establish that there is coupling. Other evidence for coupling has been presented by Goldman and Schauf (10) who found that shifts in the h_∞ curve (14) with test pulse amplitude conformed more closely to the predictions of a coupled model than to the Hodgkin and Huxley equations.

Clearly, it is important to know the time course of activation and inactivation in order to decide such questions. We describe in this paper what we think is the most direct determination of the time course of inactivation on the basis of the destruction of inactivation by pronase. It is shown that the results of pronase experiments are consistent with those derived from less direct measurements, and that all measurements suggest that activation and inactivation are not independent. The same conclusion is reached in the following paper, which describes the effect of inactivation on gating current.

MATERIALS AND METHODS

Most experiments were performed on segments of giant axons from the squid *Loligo pealei* (obtained from the Marine Biological Laboratory, Woods Hole, Mass.). A few experiments (indicated in the figure legends) were performed at the Laboratorio de Fisiología Celular, University of Chile, on *Dosidicus gigas* obtained off the coast of Chile.

To record gating currents the permeant ions must be removed on both sides of the membrane and the linear component of the capacitative current must be subtracted. The methods have been described previously (2, 3) and in this paper only modifications and improvements of the original procedure will be noted (Fig. 1*a*).

The major improvement to the apparatus was the addition of a computer (PDP8F)-connected on-line with the experimental setup. This increased the speed of data collection and allowed us to store data in the magnetic tape unit of the computer for subsequent analysis performed with the same machine. The experimental set-up, including the computer, consisted of two main sections: an analog rack and a digital rack (Fig. 1*a*).

The digital rack contained the computer with its magnetic tape units, a signal averager, and a programmable time mark generator (Devices Digitimer). The timing of pulses was controlled by the computer in conjunction with the Digitimer, which produced up to five time marks separated by adjustable intervals. The Digitimer marks were used to trigger on and off a series of pulse generators located in the analog rack. Communication between the Digitimer and the pulse generators was by way of optical isolators to prevent ground loops between the two racks.

The membrane current signal from the nerve was amplified in the analog rack and then fed into the input of the signal averager, which was under computer control. At the end of an averaging sequence the memory contents of the signal averager were

transferred to the computer memory and from there to magnetic tape. The Digitimer and the A-D converter were timed by a single crystal clock.

The signal averager is the same machine that was briefly described previously (2) and its design and characteristics have been published elsewhere (5). Three important additions have been made. (*a*) The machine is now able to substract digitally the current produced by the control pulses from the test pulse current. (*b*) Data can be taken at two

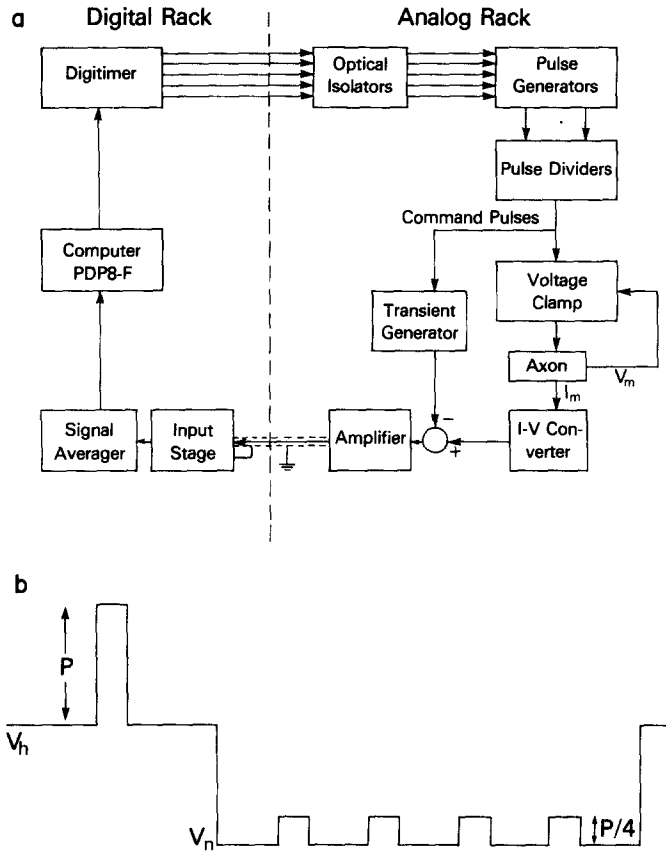

FIGURE 1. (*a*) Block diagram of the experimental set-up (for details see text). (*b*) Pulse sequence for a full cycle of the P/4 procedure. V_h is the holding potential (usually −70 mV). V_n was usually −170 mV. Duration of the cycle was normally 0.5 s. In many cases P (test pulse) was a complicated pattern and in these circumstances P/4 (control, or subtracting pulse) was the same pattern but of one-fourth the amplitude.

different sampling rates on each sweep. The first 128 points are taken at a high sampling rate (usually 10 μs per point) and the second 128 points are taken at a slower rate (usually 50 μs per point). (*c*) An input stage was placed before the sample and hold amplifier. The input stage is an operational amplifier wired as an integrator, and it integrates the input signal during the interval between samples. The period of integration is 1 μs less than the intersample interval. The gain of the integrator changes automatically when the sampling rate is switched. The effect of this integration is similar

to that of using a low pass filter, and it significantly improves the signal-to-noise ratio. It can be seen in most of the records (see, for example Fig. 1 of the following paper) that the improvement was greater (up to three times) at the low sampling rate.

P/4 Procedure

To subtract the linear portion of capacitative current from the records we used the voltage pattern of Fig. 1*b*. The current from four control or subtraction pulses of amplitude P/4 was digitally subtracted from the test pulse current. The test pulse was of amplitude P. The complete cycle was repeated 3–10 times to improve the signal-to-noise ratio, with a cycle period (usually) of 0.5 s. The method is similar to that previously described (2) but gives a better signal-to-noise ratio.

The Transient Generator

Saturation of the A-D converter by large-capacity current transients was prevented by adding in a signal from a "transient generator" (Fig. 1) as described previously (3).

As a routine, linearity tests of the apparatus were made by using an analog of the axon under voltage clamp with the same pulse patterns employed during the experiments.

Solutions

The solutions employed are listed with their composition in Table I. In the text, solutions will be referred as external solution//internal solution. Membrane voltages are not corrected for junction potentials.

Analysis of Data

Data analysis was performed with the computer (see above) by means of analysis programs that allowed us to display on an oscilloscope the original sweeps which had been recorded on magnetic tape. A short description of the different curve-fitting and analysis procedures follows.

FITTING OF THE BASE LINE Two points of the sweep were marked by cursors and a line of the form $y = ax + b$ (sloping base line) or $y = b$ (flat baseline) was fitted by use of least-squares criteria. The computer then redrew the trace relative to the fitted base line.

INTEGRATION Two selected points of the sweep were the limits of the integration, which consisted of summing the product of each data point times the duration of the sampling interval.

SINGLE EXPONENTIAL FITTING To fit a single exponential, the logarithm of each point was computed, and a linear regression was performed by taking into account the weight imposed by the process of taking logarithms (12). The fitted curve was displayed on the oscilloscope and a visual inspection of the quality of the fit was made.

DOUBLE EXPONENTIAL FITTING To fit the function $y = A \exp(-\alpha t) + B \exp(-\beta t)$, a Taylor's expansion of this function with respect to the parameters A, α, B, and β was made to linearize the equations and to find the values of these parameters for which the sum of the squares of the deviations was a minimum (12). Initial estimates of the parameters had to be provided and sometimes the convergence to a possible local minimum was tested by changing the initial estimates and observing the final convergence. Again, the goodness of the fit could be seen directly by comparing the original data and the calculated curve on the screen of the oscilloscope.

FITTING OF DOUBLE EXPONENTIAL AND BASE LINE In some cases we fitted the general function $A \exp(-\alpha t) + B \exp(-\beta t) + Ct + D$. This fitting was done also by

linearization of the general function with respect to the parameters. With this procedure no previous fitting of the base line was performed.

CONVENTIONS If one follows the usual conventions, V_m (membrane potential) is the potential inside the axon minus the potential outside. Depolarization makes V_m more positive and hyperpolarization makes it more negative. Membrane current (I) is positive when outward and negative when inward.

TABLE I
COMPOSITION OF SOLUTIONS USED

	External solutions (mM)					
Name	Na	Tris*	TMA‡	Ca	Mg	Cl
ASW	440	5		10	50	570
10% NaSW	44	401		10	50	565
20% NaSW	88	300		10	50	558
325 Na 50 Ca	325		150	50		575
40 Na 50 Ca Tris	40	447		50		587
60 Na 50 Ca Tris	60	425		50		585

	Internal solutions§ (mM)						
Name	K	Na	TMA‡	Cs	TEA-Br§	F	Glutamate
125 TMA			125			50	75
125 Cs 2 Na		2		125		127	
200 TMAFG			200			200	100
380 K 10 Na 20 TEA	380	10			20	75	315

* Tris (hydroxymethyl) aminomethane.
‡ Tetramethylammonium ion.
§ Sucrose was added to adjust osmolality to 980 mosmol/kg. 1 mM HEPES or 5 mM Tris was used as buffer. pH was adjusted to 7.1.
‖ Tetraethylammonium bromide.

RESULTS

Delayed Onset of Inactivation in Pronase Experiments

After step depolarization of an axon in a medium of low Na concentration there is an outward transient of gating current (I_g), followed by a slower inward transient of Na current (I_{Na}; Fig. 2*a*). The axon was in 10% NaSW//125 Cs 2 Na, so sodium current is small and potassium current (I_K) is absent. Trace A shows the average of current for 10 steps to 0 mV, from a holding potential (V_h) of −70 mV (see figure legend for details). After the outward gating current transient I_{Na} increases in magnitude as Na activation gates open, and then decays as the inactivation gates close.

After trace A was recorded, inactivation was destroyed by pronase applied internally for a few minutes and trace B was taken. Pronase apparently destroys some Na channels at the same time as it removes inactivation but it has no effect on the surviving activation gates as judged from the tails of sodium current during repolarization (4). To account for destruction of some channels trace B has been scaled up in amplitude by a factor of 1.3, which is the factor required to restore the gating current transient to its full amplitude. The scaling assumes that in destroying the conductance of a channel, all of its

gating current is removed. We believe that trace B, after I_g has subsided, gives a clear picture of activation gate opening, and that trace A−B, which is the difference between traces A and B, represents the closing of inactivation gates. That is, trace B shows activation gate opening, trace A−B represents inactivation gate closing, and trace A is the result of the two processes. If so, inactivation (trace A−B) follows depolarization with a definite lag. Fig. 2*b*, *c* are fits of two models to the experiment and will be discussed below.

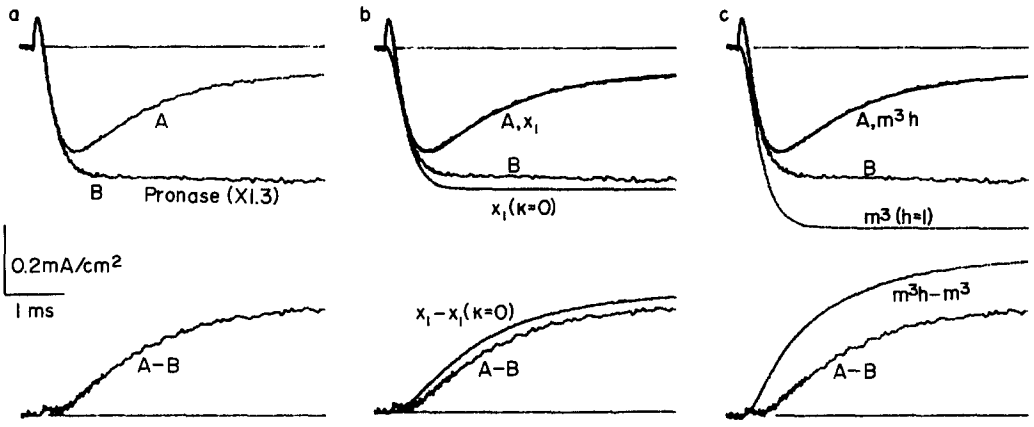

FIGURE 2. (*a*) The time course of inactivation determined with pronase. Trace A is a control record of I_g and I_{Na}, and B was recorded after 15 min of perfusion with pronase. B has been scaled up by a factor of 1.3. A − B is B subtracted from A, and it gives the time course of inactivation. A and B are sums of current from 10 cycles of the P/4 procedure, divided by 10. 70 mV pulse, from a holding potential of −70 mV. 10% NaSW//125 Cs 2 Na, 10°C. (*b*, *c*) A and B are the experimental traces described in part (*a*). The other curves are the predictions for this experiment of the model in the Discussion (*b*) or the Hodgkin and Huxley equations for I_{Na} (*c*).

Delayed Onset of Inactivation in Two Pulse Experiments

A lag in the onset of inactivation can also be demonstrated by the two pulse experiments illustrated in Fig. 3 (cf. reference 1). As shown in the diagram, a conditioning pulse to −35, −30, or −20 mV was followed after a variable interval by a test pulse to 0 mV (cf reference 13). The duration of the interval is given by the numbers in the top frame. The peak amplitude of the test current reflects the fraction of the channels that are activatable at the end of the conditioning pulse.

Only two aspects of the figure need be examined. An imaginary curve through the heavy dots gives the time course of I_{Na} during the conditioning pulse, and an imaginary envelope through the current peaks gives a good approximation of the time course of inactivation during the conditioning pulse. The envelope has a pronounced sigmoid shape, similar to trace A−B in Fig. 2. The delay of several hundred microseconds in the onset of inactivation that is evident in both figures is not predicted by the Hodgkin and Huxley equations, as discussed below.

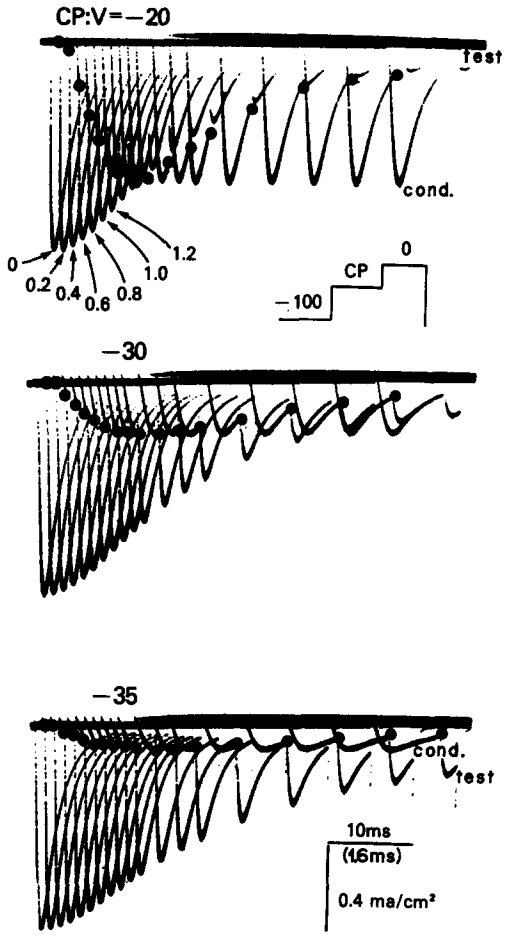

FIGURE 3. The delayed onset of inactivation demonstrated with a two-pulse procedure. The activatable fraction of the sodium conductance was determined by a test pulse to 0 mV, after conditioning pulses (CP) of different durations and amplitudes. CP duration is given by the numbers in the upper frame for which V_m during CP was −20 mV. The envelope of the test peaks gives the time course of inactivation (on the 1.6-ms time scale) and is distinctly sigmoid in shape. The heavy dots give I_{Na} at the end of each conditioning pulse, and during CP (1.6-ms time scale). It can be seen that inactivation is fastest when I_{Na} in the conditioning pulse is well developed. Details of the procedure are as follows. Each family of traces was generated by many repetitions of the pulse pattern shown in the *inset*, with a different CP duration each time. In making each photograph, a control record was first taken (no CP, trace labeled 0) at a sweep speed given by the 10-ms scale. CP duration was then increased to 0.2 ms, and the origin of the trace was shifted to the right to prevent overlap with the previous test peak. The amount of the shift was proportional to CP duration, and the appropiate time calibration is given in parentheses. Currents during the longest conditioning pulse are labeled in the upper and lower frame. Conditioning pulse current is thus shown at expanded time scale by the envelope of dots, and at compressed time scale by the labeled curves. *Dosidicus* axon injected with TEA^+ in artificial seawater. 9°C.

To a first approximation the rate of inactivation, which is given by the slope of the imaginary envelope curve, is proportional to I_{Na} (or G_{Na}) in the conditioning pulse. This suggests that the activation gate of a channel must open before inactivation can occur; the inactivation rate is roughly proportional to the number of open channels.

Further details of Fig. 3 are in the legend.

The suggestion that activation must precede inactivation is supported by Fig. 4. It has been shown that hyperpolarizing the membrane delays the turn-on of G_{Na} (2), and Fig. 4 demonstrates that inactivation is also delayed. The two curves in the figure give the amplitudes of the test currents for an experiment like that in Fig. 3, starting from $V_m = -55$ mV in one case and -140 mV in the other. (The fiber was held at -65 mV and pulsed to these values 10 ms before

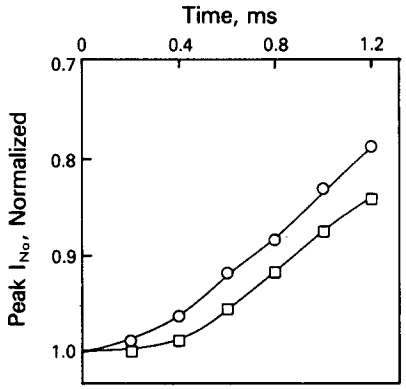

FIGURE 4. Effect of hyperpolarization on the delayed onset of inactivation. Pulse schedule as in Fig. 3. Each point is peak I_{Na} in the second pulse, normalized relative to control I_{Na} for which there was no prepulse. Circles: starting $V_m = -55$ mV. Squares: starting $V_m = -140$ mV. Axon injected with 450 CsF and 100 TEA-Br and bathed in ASW. 2°C.

the beginning of a conditioning pulse to -30 mV. Inactivation, like activation [not illustrated] is delayed by hyperpolarization, which again suggests that activation must precede inactivation. It must be noted, however, that the delay for activation and that for inactivation have not been measured at the same potential.)

Other Measures of Inactivation Time Course

In the preceding sections we examined the time course of inactivation by using a one-pulse method (the pronase experiments of Fig. 2) and a two-pulse method (Fig. 3). It has been stated, however, that the one-pulse and two-pulse methods give different results for the time course of inactivation. Goldman and Schauf (11), using *Myxicola* axons, reported that τ_h, the time constant of inactivation measured from the decay of I_{Na} after a single pulse, differs from that measured with a two-pulse method. The latter time constant they called τ_c. They found the difference to be most pronounced from -30 to -50 mV. As

V_m is made negative in this range, τ_c increases steeply but τ_h is, in *Myxicola*, much less voltage dependent than τ_c. Hodgkin and Huxley (using squid axons) originally reported that τ_c and τ_h have the same value, and that τ_h is just as voltage dependent near −40 mV as τ_c. This is clearly a question of importance, and we consequently repeated these experiments and obtained the results shown in Fig. 5, which are in good agreement with those of Hodgkin and Huxley.

The axons represented were bathed in solutions with low Na concentration, and I_K was eliminated by replacing internal K^+ with TMA^+. The falling phase of each I_{Na} transient was fitted with a single exponential (sometimes two exponentials would have been a better fit, cf. reference 8) by a least-squares

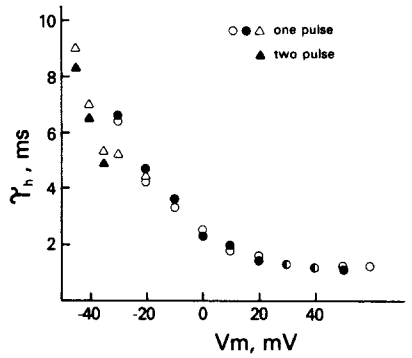

FIGURE 5. Time constant of inactivation. For the one-pulse method (see *inset* for symbols), the time constant of decay of I_{Na} (τ_h) (see text) is plotted as a function of V_m during the test pulse (open symbols). In the two-pulse method (see *inset*, Fig. 3) peak I_{Na} during the second pulse (to V_m = 20 mV) was plotted semilogarithmically as a function of the duration of the first pulse and a time constant τ_c was obtained. τ_c is given by the filled triangles. Axons were in 40 Na 50 Ca//200 TMA. Each symbol represents a different axon. Holding potential was −70 mV for circles and −100 mV for triangles. P/4 procedure. 8°C.

method, and the results are given in Fig. 5. In all three experiments τ_h is a steep function of voltage near −30 to −40 mV.

In two experiments, both τ_c and τ_h were measured and compared in the voltage range near −40 mV, and the results are shown in Fig. 5 and Table II. If anything, τ_h tends to be slightly slower than τ_c but the difference is probably not significant.

The major difference between the *Myxicola* and squid results is, as noted, in the time course of I_{Na} for depolarizations to about −40 mV; in squid, inactivation after a single pulse is quite slow in this voltage range. This is illustrated in Fig. 6, for an axon in 325 Na 50 Ca//380 K 10 Na 20 TEA. At −40 mV, inactivation is so slow that it is not apparent by the end of the trace.

Inactivation as a Function of V_m

Steady-state inactivation of the Na channels increases with membrane voltage in the range −70 to 0 mV (13, 14), but it then decreases again at large positive

voltages (6). This phenomenon is illustrated in Fig. 6 for an axon with 10 mM Na inside: for the depolarization to +80 mV, steady-state I_{Na} is approximately one-third of the peak value. The findings of Chandler and Meves (6) suggested to us that inactivation might be affected by current flow through the channel and be less complete for large outward currents. We investigated this question by determining steady-state inactivation in axons with no Na^+ inside. To do

TABLE II

INACTIVATION TIME CONSTANTS FOR TWO METHODS

	Time constant, (ms)		
V_m	one pulse	two pulse	Temperature
			°C
−45	9.0	8.3	8
−40	6.9	6.5	8
−35	5.3	4.9	8
−45	3.1	2.5	15
−40	2.6	2.1	15
−35	1.9	1.8	15

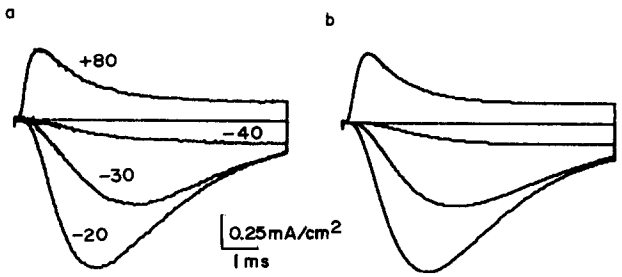

FIGURE 6. Time course of I_{Na} as a function of potential. (*a*) Experimental traces. The numbers indicate the potential during the test pulse. Each trace is the result of the current obtained in 325 Na 50 Ca//380 K 10 Na 20 TEA minus the current obtained in the same solutions with TTX added. P/4 procedure. Series resistance compensation 4 Ωcm^2. 2°C. (*b*) Sodium currents predicted by the model presented in the Discussion. Each trace has been calculated for the corresponding membrane potential indicated in part (*a*) and with the parameters listed in Table IV.

this, V_m was returned to −60 mV after a long pulse and tail current was measured just after the step back and plotted as a function of V_m during the preceding pulse. For comparison and normalization purposes, tail current was also measured when the step was interrupted at the peak of the I_{Na} transient, and these currents are plotted in Fig. 7, normalized relative to the largest tail current. This curve shows the usual behavior of peak G_{Na} as a function of V_m: it rises along a sigmoid curve, and saturates at about +20 mV. Currents after long pulses were normalized in the same way and are given by the curve with filled circles in the figure. This curve rises relatively slowly to about +10 mV and then more steeply. At +90 mV, steady state G_{Na} is 43% of its maximum value. We conclude that inactivation can be incomplete in the absence of internal Na and outward I_{Na}, and that Chandler and Meves were correct in

ascribing incomplete inactivation to a voltage-dependent rather than a current-dependent process.

Steady-state inactivation was also studied by a two-pulse method (Fig. 8,

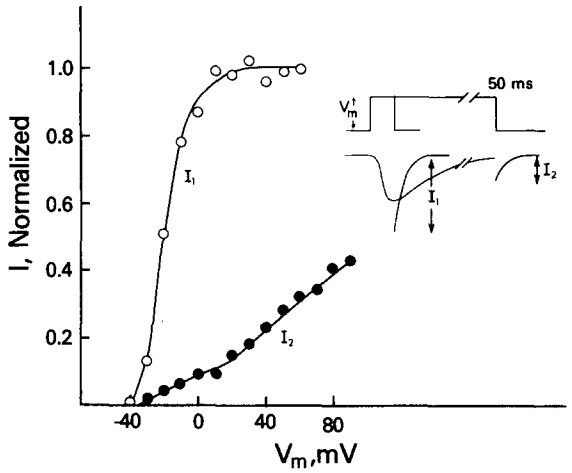

FIGURE 7. Inactivation as a function of V_m as measured with tails. The pulse procedure is shown in the *inset*. I_1 was determined at the peak of I_{Na} and I_2 at the end of a 50 ms pulse. TTX-insensitive currents were subtracted off before I_1 and I_2 were determined. Both I_1 and I_2 have been normalized relative to the maximum tail current obtained at peak I_{Na}. Axon in 60 Na 50 Ca//200 TMA. Holding potential, −70 mV. P/4 procedure. 8°C.

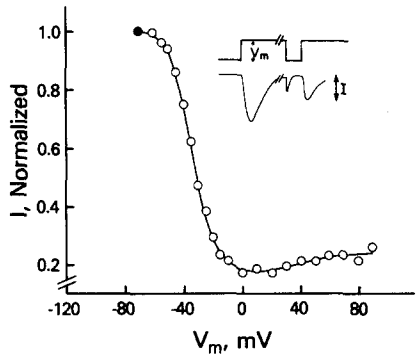

FIGURE 8. Inactivation as a function of V_m as determined with a double-pulse method. The pulse procedure is indicated in the *inset*. *I* is plotted as a function of V_m during the first pulse (see *inset*), and it has been normalized relative to I_{Na} for which there was no first pulse (filled circle). TTX-insensitive currents were subtracted off before *I* was measured. Holding potential, −70 mV. The first pulse was 40 ms long and at the end V_m was returned to −70 mV for 0.7 ms. The second pulse took V_m to 30 mV. Axon in 60 Na 50 Ca//200 TMA. P/4 procedure. 8°C.

inset), which gave an initially surprising result. The second pulse was of fixed amplitude, while the first was variable. The plot in Fig. 8 gives the peak amplitude of I_{Na} during the second pulse as a function of V_m during the first. The points have been normalized relative to I_{Na} for which there was no first

pulse, the filled circle. Between −70 and 0 mV the points follow the usual sigmoid curve, with a midpoint at about −30 mV. Beyond 0 mV the curve is almost flat, with a slight upward turn near +60 mV. Measured in this way, steady-state inactivation is about 80% and is almost independent of V_m above 0 mV, quite unlike the results from Figs. 6 and 7. The difference in the two methods can be reconciled by the Chandler and Meves (6) model for a second activated state, as discussed below.

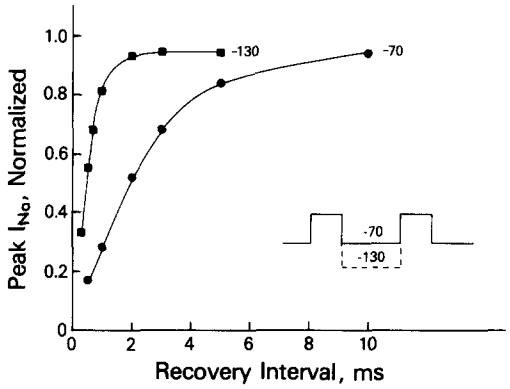

FIGURE 9. Time course of recovery from inactivation. These curves represent peak I_{Na} (plotted as the fraction of peak I_{Na} without prepulse) as a function of the recovery interval between the prepulse and the test pulse (see *inset*). Prepulse and test pulses took V_m to 10 mV. Solid symbols: recovery at −70 mV. Open symbols: recovery at −130 mV. Prepulse duration: 10 ms. P/4 procedure. The axon was in 20% NaSW//125 TMA. 8°C.

Recovery from Inactivation

Inactivation gates open when membrane potential is restored to a negative value after a depolarization. This process has been called recovery from inactivation and its time course can be studied with two depolarizing pulses separated by a variable interval, as drawn in the inset of Fig. 9. The first pulse must be long enough to develop inactivation, and the second pulse is given to test the amount of Na conductance available after the recovery interval which is a variable. Fig. 9 shows that inactivation recovery has an approximately exponential time course that is voltage dependent. At −70 mV the time constant of recovery is 2.7 ms and it decreases to 0.6 ms at V_m = −130 mV. Voltage dependence of the recovery rate is not a new finding but we know of no reported observations at very negative voltages.

DISCUSSION

The major findings of this paper are that inactivation begins with a lag after depolarization, and that the time course of inactivation is the same whether measured with a one-pulse or a two-pulse method. The lag, which has been detected before (1, 10), has now been demonstrated by two methods: by the conditioning pulse experiment (Fig. 3); and by destroying inactivation with pronase (Fig. 2). With the two-pulse method, the lag is evident only for

conditioning pulses of very short duration. It is therefore not surprising that a lag was not observed by Hodgkin and Huxley (13) in their original description of inactivation, for the shortest prepulse they used was 2 ms.

Rather surprisingly, the time course of inactivation is not well known in spite of considerable theoretical work regarding the mechanism of the phenomenon. The problem, of course, is that the kinetics of I_{Na} are determined by two gating factors, and the behavior of neither is known in detail. In our view, the pronase experiment of Fig. 2 provides the most straightforward measure of the time course of inactivation, despite the uncertainty introduced by the necessity to scale the post-pronase record to make up for destruction of some Na channels. In addition to confirming the existence of a lag, the pronase experiment shows (if the scaling is correct) that a large fraction of the Na channels can be simultaneously active after a large depolarization. In the Hodgkin and Huxley equations, there is considerable overlap between activation and inactivation and, in consequence, the number of conducting channels after depolarization is a rather small fraction of the total. For Hodgkin and Huxley's axon 17, for example, only 43% of the channels are open at the peak of the transient even for a very large pulse with $h_0 = 1$ (14). The experiment of Fig. 2 suggests that Na channels are used much more efficiently than the Hodgkin and Huxley equations predict, and that 70% or 80% of them can be open at the peak of the I_{Na} transient.

In our hands, the time course of inactivation is the same whether measured with a one pulse or a two pulse method, and this is in agreement with previous results from squid (14) and myelinated frog fibers (Chiu, personal communication). In these preparations there is no distinction between τ_h and τ_c, unlike the situation in *Myxicola* (11) and lobster (18).

The lag in the onset of inactivation and the accentuation of this lag by hyperpolarization (Fig. 4) suggest that the activation gates of an Na channel must open before the inactivation gate can close. Gating current experiments reported in the next paper strongly support this idea, and provide the main impetus for the following model, which describes the possible states of a sodium channel,

$$x_5 \underset{b_4}{\overset{a_4}{\rightleftharpoons}} x_4 \underset{b_3}{\overset{a_3}{\rightleftharpoons}} x_3 \underset{b_2}{\overset{a_2}{\rightleftharpoons}} x_2 \underset{b_1}{\overset{a_1}{\rightleftharpoons}} x_1 \underset{\lambda}{\overset{\kappa}{\rightleftharpoons}} x_1 z \underset{\pi}{\overset{\epsilon}{\rightleftharpoons}} h_2 .$$

The model is expanded in the next paper to account for gating current phenomena. There are four closed states, x_5–x_2; two open states x_1, h_2; and one inactivated state $x_1 z$. The conductance of the closed and inactivated states is zero. Both open states are postulated to have the same conductance, roughly 10^{-11} S per channel (9, 17, 18).

Four sets of calculations have been performed to match the model to experimental findings. The computations must be regarded as preliminary, for inactivation is linked to activation in the model and cannot be described accurately without more knowledge regarding activation than is presently at hand. Specifically, in the terms of this model, it is necessary to specify the rate constants a_1–a_4 and b_1–b_4, and this was done as follows:

$$x_4 \underset{b}{\overset{a}{\rightleftharpoons}} x_3 \underset{b}{\overset{a}{\rightleftharpoons}} x_2 \underset{b}{\overset{a}{\rightleftharpoons}} x_1 \underset{\lambda}{\overset{\kappa}{\rightleftharpoons}} x_1 z \underset{\pi}{\overset{\epsilon}{\rightleftharpoons}} h_2$$

That is, it was assumed that all of the forward rate constants for the activation process are equal, and similarly for the backward rate constants. State x_5 is populated only at very negative voltages and was omitted. No attempt was made to simulate gating current. The main purposes of the calculations are to show, by the simplest model possible, that activation and inactivation may be coupled and that the inactivation step need not be significantly voltage dependent. Both points are supported by evidence from gating current studies that are reported in the next paper.

TABLE III

PARAMETERS OF THE CURVES IN FIG. 2*b*, *c*

Curve	a	b	κ	λ	$\bar{I}$
	ms^{-1}	ms^{-1}	ms^{-1}	ms^{-1}	mA/cm^2
y*	8	0	0.65	0.12	−0.42
y ($\kappa = 0$)*	8	0	0	0	−0.42
Curve	α_m	β_m	α_h	β_h	$\bar{I}$
	ms^{-1}	ms^{-1}	ms^{-1}	ms^{-1}	mA/cm^2
m^3h	5	0	0.108	0.692	−0.53
m^3	5	0	1	0	−0.53

* For these calculations, $\epsilon = \pi = 0$.

Membrane current was calculated from the equation

$$I_m = x_1 \bar{I},$$

where

$$\bar{I} = \bar{G}_{Na} (V - V_{Na}).$$

$\bar{I}$ is the current that would flow for a given driving force $(V - V_{Na})$ if all channels were open simultaneously; and $\bar{G}_{Na}$ (14) is the conductance of an open channel times the total number of channels.

The first calculation is a fitting of the model to the experiment of Fig. 2, and the rate constants and other parameters determined are given in Table III. Trace A was fitted first (less the gating current), yielding the theoretical curve labeled x_1. Rate constant κ was then set to zero to stimulate removal of inactivation by pronase, and curve x_1 ($\kappa = 0$) was calculated. Finally, the two computed curves were subtracted from each other to give the lower curve, $x_1 - x_1$ ($\kappa = 0$). Overall, the fits are reasonably good. There is a prominent lag in the onset of inactivation (that is, $x_1 - x_1$ ($\kappa = 0$) is sigmoid), and the peak value of curve x_1 is 73% of the final level of current in the curve x_1 ($\kappa = 0$); i.e. a rather large fraction of the channels are open at the peak of curve x_1. A somewhat better fit can be obtained with the more complex model of the next paper which predicts a longer lag in activation and a larger open fraction of channels at the peak of the normal current transient.

The Hodgkin and Huxley equations give a relatively poor fit to this experiment as shown in Fig. 2*c* (parameters are given in Table III). The m^3h curve

conforms closely to trace A, but fixing h at 1.0 to simulate removal of inactivation by pronase yields a curve (m^3) that is far larger in amplitude than trace B. The curve m^3h-m^3 is also a poor fit to trace A−B, and has an initial lag that is much smaller than that experimentally observed.

The second calculation fits the model to the I_{Na} transients in Fig. 6*a*. The results of the fit are given in Fig. 6*b*, and the parameters are in Table IV. $\bar{I}$ was set by assuming a linear instantaneous current voltage curve below the sodium equilibrium potential and a curve with lesser slope (by a factor of 0.72) above V_{Na}. The time constant of the step $x_1z \rightleftharpoons h_2$ was taken from Chandler and Meves (7) and scaled to 8°C by using a Q_{10} of 3. A point of particular interest is that good fits are obtained even though the rate constant of inactivation (κ) shows no systematic variation with voltage. The overall rate of inactivation is strongly affected by voltage, as is τ_h (14); but it is quite possible that most or all of this voltage dependence arises from coupling to the activation process ($x_4 \rightleftharpoons x_1$), as Fig. 6*b* shows. Gating current measurements in the next paper also suggest that the forward rate constant of inactivation is not significantly voltage dependent.

TABLE IV
PARAMETERS OF THE THEORETICAL CURVES IN FIG. 6*b*

V_m	a	b	κ	λ	ϵ	π	$\bar{I}$
mV	ms^{-1}	ms^{-1}	ms^{-1}	ms^{-1}	ms^{-1}	ms^{-1}	mA/cm^2
−40	0.5	0.88	0.8	0	0	0	−4.15
−30	1.0	0.4	1.1	0	0	0	−3.74
−20	1.67	0.4	0.8	0	0.075	1.9	−3.32
+80	9.0	0	0.83	0	0.35	1.4	0.60

The third calculation shows that the model predicts a reasonable facsimile of the h_∞ curve (14). The values of a and b were selected to reproduce the m_∞^3 that is implied by Fig. 8 of Hodgkin and Huxley (14). This curve (labeled m_∞^3, x_1) is plotted in Fig. 10, together with the h_∞ curve from Fig. 9 of Hodgkin and Huxley (14) on the assumption that the resting potential in their experiments was −60 mV. The calculation was performed by setting

$$x_4+x_3+x_2+x_1+x_1z = 1, x_5 = h_2 = 0,$$

and determining the distribution among the various states for the selected values of a and b. Curves of $1-x_1z$ are plotted for three values of κ/λ. The curve for κ/λ = 1,000 is the best fit to the h_∞ curve although it is somewhat too steep, particularly in the range −60 to −70 mV, and it saturates near −70 rather than −100 mV. Neither of these defects seems very serious since the calculated curve depends on the ratio of a to b, and this ratio, like m_∞^3 from which it is derived, cannot be accurately determined in the voltage range negative to −50 or −60 mV. The curve also depends on the activation rate constants, which may not have the values that have been assumed.

The fourth computation, which is not illustrated, shows that τ_c and τ_h are the same for this model, as would be expected, since by either of the experimental procedures inactivation rate is proportional to the number of channels in state x_1.

Two other attributes of the model can be appreciated without the need for calculation, and these are the effects of states x_5 and h_2. State x_5 is included to account for the increased lag in both activation and inactivation caused by hyperpolarization. If most of the channels are in state x_4 at −70 mV and in state x_5 at −150 mV, the lag will be longer for a step beginning from the more negative voltage. (It is likely that state x_5 should in fact be several states to provide the necessary lag.)

State h_2 is the second activated state postulated by Chandler and Meves (6) and is included here to explain the high steady-state value of G_{Na} (sodium conductance) for large voltages. State h_2 is favored at large positive V_m. It was shown above that steady-state inactivation at large V_m seems incomplete when

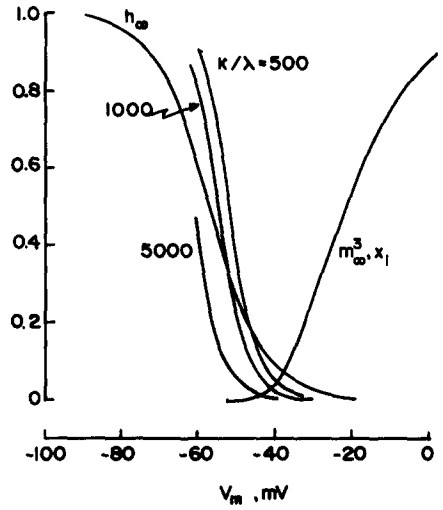

FIGURE 10. Inactivation as predicted by the coupled model. Curve labeled h_∞ is from Fig. 9 of Hodgkin and Huxley (1952*b*). Steady-state inactivation curves were calculated with the model presented in the discussion and represent $1 - x_1z$ for κ/λ = 500, 1,000, and 5,000. m_∞^3, x_1 is the m_∞^3 curve of Hodgkin and Huxley (1952*b*). This curve was fitted with the model to give the ratio a/b, which was used in calculating $1 - x_1z$.

measured from the I_{Na} tail after a large pulse (Fig. 7), but is much more complete when determined by a two-pulse method (Fig. 8). This can be explained as follows. At the end of a very large pulse, about one-third of the channels are in state h_2, and they contribute to steady-state I_{Na} and the I_{Na} tail at pulse end. After a fraction of 1 ms at −60 or −70 mV, all of these channels have reverted from state h_2 to the inactivated state x_1z, and they can conduct again when V_m is pulsed to 30 mV (as in Fig. 8) only after recovery from inactivation. So after ~0.5 ms at −70 mV, most of the channels are in state x_1z regardless of whether the first pulse was large or very large. Steady-state inactivation thus seems independent of pulse size (for large pulses) when determined with a two-pulse method.

The common impression that inactivation can occur without preceding activation seems to speak against the model proposed here. This impression

must be based more on a literal interpretation of the Hodgkin and Huxley equations than on observation, for we are aware of no evidence to support it. In Fig. 3 inactivation is preceded by easily measurable activation during the conditioning pulse. At more negative voltages it is clear that significant activation must also occur, as is evident from the phenomenon of anodal break excitation: a fiber that is hyperpolarized by a long pulse of current may generate an action potential when the current is turned off. In such a case enough Na channels open to initiate the action potential even when V_m is negative to the normal threshold.

The model given here predicts a small sodium current during recovery from inactivation, as channels reflux through state x_1z before closing. This current has not been observed, and is not predicted by the more complex model of the next paper.

This work was supported by United States Public Health Service grant no. NS 08951.

Received for publication 24 January 1977.

REFERENCES

1. ARMSTRONG, C. M. 1970. Comparison of g_k inactivation caused by quaternary ammonium ion with g_{Na} inactivation. *Biophys. J.* **10**(2, Pt. 2):185*a*. (Abstr.).
2. ARMSTRONG, C. M., and F. BEZANILLA. 1974. Charge movement associated with the opening and closing of the activation gates of the Na channels. *J. Gen. Physiol.* **63**:533–552.
3. ARMSTRONG, C. M., and F. BEZANILLA 1975. Currents associated with the ionic gating structures in nerve membrane. *Ann. N. Y. Acad. Sci.* **264**:265–277.
4. ARMSTRONG, C. M., F. BEZANILLA, and E. ROJAS. 1973. Destruction of sodium conductance inactivation in squid axons perfused with pronase. *J. Gen. Physiol.* **62**:375–391.
5. BEZANILLA, F., and C. M. ARMSTRONG. 1977. A low cost signal averager and data acquisition device. *Am. J. Physiol.: Cell Physiol.* **1**(3):C211–C215.
6. CHANDLER, W. K., and H. MEVES. 1970. Evidence for two types of sodium conductance in axons perfused with sodium fluoride solution. *J. Physiol. (Lond.).* **211**:653–678.
7. CHANDLER, W. K., and H. MEVES. 1970. Rate constants associated with changes in sodium conductance in axons perfused with sodium fluoride. *J. Physiol. (Lond.).* **211**:679–705.
8. CHIU, S. Y. 1976. Observations on sodium channel inactivation in frog nerve. *Biophys. J.* **16**(2, Pt. 2):25*a*. (Abstr.).
9. CONTI, F., L. J. DEFELICE, and E. WANKE. 1975. Potassium and sodium current noise in the membrane of the squid giant axon. *J. Physiol. (Lond.).* **248**:45–82.
10. GOLDMAN, L., and C. L. SCHAUF. 1972. Inactivation of the sodium current in *Myxiola* giant axons. Evidence of coupling to the activation process. *J. Gen. Physiol.* **59**:659–675.
11. GOLDMAN, L., and C. L. SCHAUF. 1973. Quantitative description of sodium and potassium currents and computed action potentials in *Myxicola* giant axons. *J. Gen. Physiol.* **61**:361–384.
12. GUEST, P. B. 1961. Numerical methods of curve fitting. Cambridge University Press, Cambridge.

13. HODGKIN, A. L., and A. F. HUXLEY. 1952. The dual effect of membrane potential on sodium conductance in the giant axon of *Loligo*. *J. Physiol.* (*Lond.*). **116**:497–506.
14. HODGKIN, A. L., and A. F. HUXLEY. 1952. A quantitative description of membrane current and its application to conduction and excitation in nerve. *J. Physiol.* (*Lond.*). **117**:500–544.
15. HOYT, R. C. 1965. The squid giant axon: mathematical models. *Biophys. J.* **3**:399–431.
16. HOYT, R. C. 1968. Sodium inactivation in nerve fibers. *Biophys. J.* **8**:1074–1097.
17. KEYNES, R. D., E. ROJAS, and R. E. TAYLOR. 1973. Saxitoxin, tetrodotoxin barriers, and binding sites in squid giant axons. *J. Gen. Physiol.* **61**:267.
18. NONNER, W., F. CONTI, B. HILLE, B. NEUMCKE, and R. STÄMPFLI. 1976. Current noise and the conductance of single Na channels. *Pfluegers Arch. Eur. J. Physiol.* **362,** R27.
19. OXFORD, G. S., and J. P. POOLER. 1975. Selective modification of sodium channel gating in lobster axons by 2,4,6-trinitrophenol. Evidence for two inactivation mechanisms. *J. Gen. Physiol.* **66**:765–779.